# Modeling of Nonlinear Active Regions with the FDTD Method

B. Toland, *Member, IEEE*, B. Houshmand, *Member, IEEE*, and T. Itoh, *Fellow, IEEE*

***Abstract*—The FDTD method is extended to include nonlinear active regions embedded in distributed circuits. The procedures necessary to produce a stable algorithm are described, and a single device cavity oscillator is simulated with this method.**

## I. Introduction

RECENTLY, the two-dimensional FDTD method was extended to include active, passive and possibly nonlinear lumped circuit elements [1]. In that work the incorporation of the lumped elements into the FDTD algorithm is described, and transmission lines with various lumped element loads were simulated. Only one active load was modeled, which was linear, and this was modeled in the same fashion as the passive lumped elements. However, we have found that to accurately model active nonlinear regions requires some extra steps and precautions which are not necessarily needed for passive element modeling. Some of these precautions have been noted in [2], in which active nonlinear circuit models were incorporated into the TLM method.

For instance, in [2] the TLM method was used to model active nonlinear subregions of distributed circuits, and it was noted that regions of negative conductivity may cause spurious oscillations at the TLM mesh cut-off frequencies. To circumvent this problem, the TLM mesh cut-off is chosen to be well above the active device cut-off frequency. It is therefore not too surprising that to avoid spurious oscillations at the FDTD mesh cut-off frequency, the FDTD mesh cut-off frequency must be well above the active device cut-off frequency. In addition, we have found that in many cases the FDTD algorithm will become unstable unless some care is taken in incorporating the active device model into the FDTD method. This is because a realistic active device can produce extremely large local currents which produce large fields that are fed back into the device model that can create a "runaway" effect.

The purpose of this letter is to describe the steps we have implemented to produce a stable algorithm which simulates realistic devices with both active and nonlinear regions. We use this algorithm to simulate a single device cavity oscillator. The device is both nonlinear and active, and the nonlinear active region is distributed over more than one cell.

Manuscipt received May 25, 1993. This work was supported by JSEP Contract F49620-92-C-0055 and the Office of Naval Research Contract N0014-91-J-1651 and Army Research Office Contract DAAH04-93-G-0068. Editorial decision made by S. Maas.

The authors are with the department of Electrical Engineering, University of California, Los Angeles, 66-147A Engineering IV, 405 Hilgard Avenue, Los Angeles, CA 90024-1594.

IEEE Log Number 9211895.

## II. Incorporation of the Active Device Model into the FDTD Algorithm

The active device which we will model is a resonant tunneling diode (RTD) which was fabricated at UCLA. The equivalent circuit and IV characteristic are shown in Fig. 1. The junction capacitance $C$, series resistance $R$ and nonlinear current source $F(V_s)$ are converted into distributed parameter values $\overline{R}, \overline{C}$ and $\overline{F(V_s)}$ which will be used for each mesh cell in the packaged device volume. This is done so that each cell in the active region is a voltage source, with the aggregate effect of all cells in the active region representative of the physical device. Note also that we subtract out the dc bias point from the voltages and currents, i.e., $V_s$ and $F(V_s)$ are with respect to the bias point. Voltage or current sources can be included into the FDTD algorithm as described in [1], but with the following additional steps to ensure a stable algorithm. For the device shown in Fig. 1, the voltage source is a solution of

$$\frac{dV_s}{dt} + \frac{V_s}{RC} + \frac{F(V_s)}{C} = \frac{-V_y}{RC}. \tag{1}$$

To solve this equation, we use forward time average differencing [3]. This requires that we expand the nonlinear current source in a Taylor series [4]:

$$F(V_s^{n+1}) \approx F(V_s^n) + \frac{dF(V = V_s^n)}{dV}[V_s^{n+1} - V_s^n]. \tag{2}$$

We then obtain the finite difference form of (1), which is

$$V_s^{n+1} = A_1 V_s^n - A_2 F(V_s^n) - A_3 \Delta y [E_y^{n+1} + E_y^n], \tag{3}$$

where

$$A_1 = \frac{2RC - \Delta t[1 - R\dot{F}(V_s^n)]}{\beta}, A_2 = \frac{2R\Delta t}{\beta}, A_3 = \frac{\Delta t}{\beta} \tag{4}$$

with $\beta = 2RC + \Delta t[1 + R\dot{F}(V_s^n)]$ and $\dot{F}(V_s^n) = \frac{dF(V=V_s^n)}{dV}$. This can be put back into the FDTD algorithm which is of the forward time average form as in [1]. Since we are considering a y-directed source, we have the following for the $E_y$ component:

$$E_y^{n+1} = E_y^n \frac{\left[\frac{\varepsilon}{\Delta t} - \frac{1}{2\overline{R}}(1 - A_3)\right]}{\left[\frac{\varepsilon}{\Delta t} + \frac{1}{2\overline{R}}(1 - A_3)\right]} + \frac{H_x^{n+1/2}(i, j + 1/2, k + 1/2) - H_x^{n+1/2}(i, j + 1/2, k - 1/2)}{\Delta z\left[\frac{\varepsilon}{\Delta t} + \frac{1}{2\overline{R}}(1 - A_3)\right]}$$

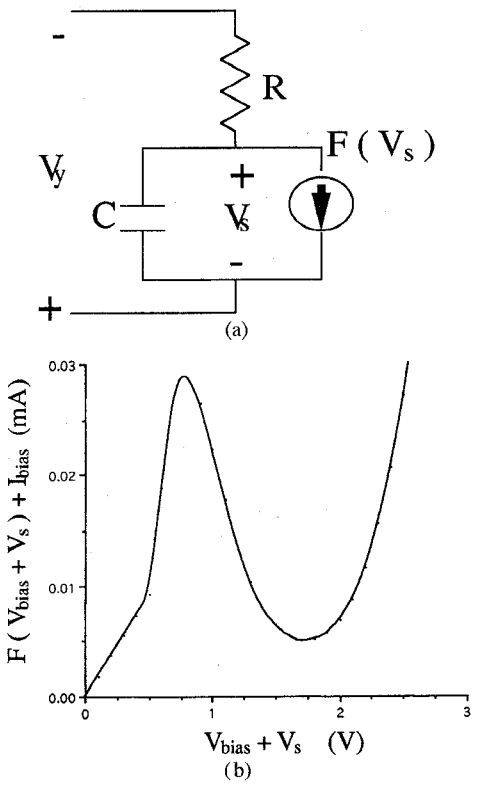


Fig. 1. Circuit model of resonant tunnelling diode and IV characteristic.

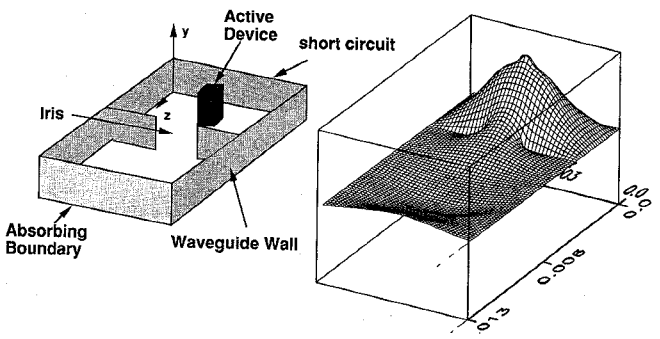


Fig. 2. The layout of the waveguide oscillator and the steady-state electric field distribution at one instant in time.

$$- \frac{H_z^{n+1/2}(i+1/2,j+1/2,k) - H_z^{n+1/2}(i-1/2,j+1/2,k)}{\Delta x\left[\frac{\varepsilon}{\Delta t} + \frac{1}{2\overline{R}}(1-A_3)\right]} - \left[\frac{(1+A_1)V_s^n - A_2F(V_s^n)}{2\overline{R}\Delta y\left[\frac{\varepsilon}{\Delta t} + \frac{1}{2\overline{R}}(1-A_3)\right]}\right]. \quad (5)$$

$E_y$ is evaluated at the point $(i, j+1/2, k)$( Yee's notation [5]). By using (3) in conjunction with (5), instabilities have been eliminated from all tunnel diode cases that we have considered.

## III. Modeling of a Single Device Cavity Oscillator

In this section, we describe the FDTD simulation of a reduced height WR28 waveguide cavity oscillator shown in Fig. 2. The RTD parameter values of $C = 0.05$ pF, $R = 9.7\ \Omega$ and an extrapolated polynomial fit for $F(V_{bias} + V_s)$ (see Fig. 1) were used [6]. At the bias point of $V_{\text{bias}} = 1.25$ V, $I_{\text{bias}} = 11.86$ mA the small signal conductance $G = \dot{F}(V_{\text{bias}}) = -32.5$ m $\Omega^{-1}$ and the diode cut-off frequency is 152 GHz. The mesh sizes were $\Delta x = \Delta z = 0.17775$ mm. The cavity width is $40\Delta x$, the distance between the backshort and inductive iris is $22\Delta z$, and the diode covers 6 cells and is centered in the cavity. The symmetrical, perfectly conducting iris has zero thickness, an aperture $12\Delta x$ wide, with the waveguide 5.0 mm high.

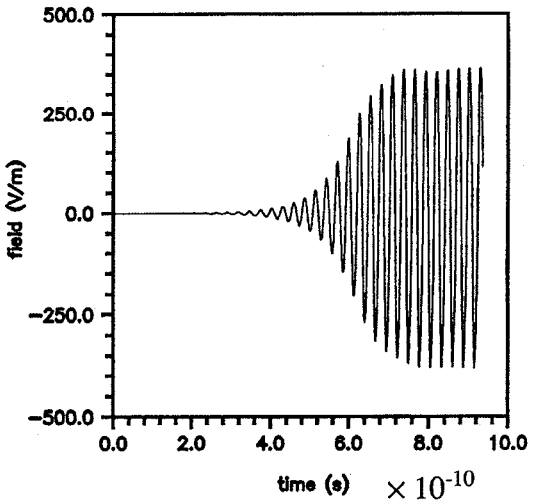


Fig. 3. The time development of the electric field $E_y$ at anobservation point outside the resonant cavity.

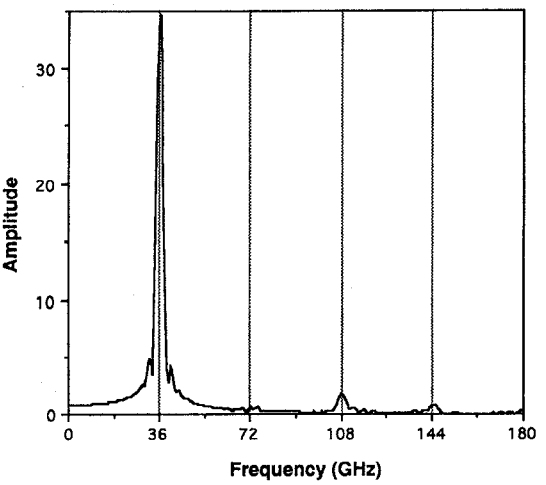


Fig. 4. The frequency spectrum of the steady-state electric field.

In Fig. 2, we show the layout of the oscillator and the steady state electric field distribution $E_y$ at one instant in time. Fig. 3 is a plot of the electric field vs. time at an observation point outside the cavity. A small amount of "noise" is introduced into the cavity, and the oscillations build up with time until saturation occurs. In Fig. 4, we show the corresponding spectrum of the oscillator in the steady state (a fifth-order polynomial was used to model the NDR region of the RTD). Both spurious oscillations at the mesh cut-off frequency and algorithm instabilities have been suppressed with this algorithm and by modeling the correct physical behavior of the active device.

## IV. Conclusion

A FDTD algorithm that simulates distributed circuits containing nonlinear active elements has been described, and a single device cavity oscillator has been modeled. The additional steps necessary to obtain a stable algorithm that simulates a realistic active device embedded in a distributed circuit have been described. An application of the algorithm described in this paper can be applied to a number of circuits which have been characterized by the harmonic balance method. However, the present method has the advantage in that the passive planar structures, including discontinuities, can be handled without resorting to the equivalent circuits which are used in the harmonic balance method.

## Acknowledgment

The authors are grateful to O. Boric for for providing us with the RTD parameters. The authors would also like to thank T.-W. Huang, R. Chan, and M. Jensen for their advice and encouragement.

## References

[1] W. Sui, D. A. Christensen, and C. H. Durney, "Extending the two-dimensional FDTD method to hybrid electromagnetic systems with active and passive lumped elements," *IEEE Trans. Microwave Theory Tech.*, vol. 40, no. 4, pp. 724–730, Apr. 1992.

[2] P. Russer, P. M. So, and W. J. R. Hoefer, "Modeling of nonlinear active regions in TLM," *IEEE Microwave Guided Wave Lett.*, vol. 1, no. 1, pp. 10–13, Jan. 1991.

[3] L. Lapidus and G. F. Pinder, *Numerical Solution of Partial Differential Equations in Science and Engineering*. New York: John Wiley, 1982.

[4] W. H. Press, B. P. Flannery, S. A. Teukolsky, and W. T. Vetterling, *Numerical Recipes*. New York: Cambridge Univ. Press, 1986.

[5] K. S. Yee, "Numerical solution of initial boundary value problems involving Maxwell's equations in isotropic media," *IEEE Trans. Antennas Propagat.*, vol. AP-14, no. 3, pp. 302–307, May 1966.

[6] O. Boric-Lubecke, private communication.